PLANT SCIENCE TODAY
ISSN 2348-1900 (online)
Vol x(x): xx–xx
https://doi.org/10.14719/pst.2180

HORIZON
e-Publishing Group
HePG

RESEARCH ARTICLE

Identification and authentication of *Agnimantha* plant species used in Ayurveda on the basis of anatomical and molecular phylogenetic analysis

Anurag Kumar[#1], Prem Prakash Jangid[#1], S. Marimuthu[1], Arun.M.Gurav[*1], N. Srikanth[2], Anupam K. Mangal[2], B. Venkateshwarlu[2] & N. Shiddamallayya[2]

[1]Regional Ayurveda Research Institute, Pune, India
[2]Central Council for Research in Ayurvedic Sciences, New Delhi, India

***Email:** gurav_am@yahoo.co.in

OPEN ACCESS

ARTICLE HISTORY
Received: 11 October 2022
Accepted: 11 May 2023
Available online
Version 1.0 : 21 August 2023

Check for updates

Additional information

Peer review: Publisher thanks Sectional Editor and the other anonymous reviewers for their contribution to the peer review of this work.

Reprints & permissions information is available at https://horizonepublishing.com/journals/index.php/PST/open_access_policy

Publisher's Note: Horizon e-Publishing Group remains neutral with regard to jurisdictional claims in published maps and institutional affiliations.

Indexing: Plant Science Today, published by Horizon e-Publishing Group, is covered by Scopus, Web of Science, BIOSIS Previews, Clarivate Analytics, NAAS,UGC Care etc. See https://horizonepublishing.com/journals/index.php/PST/indexing_abstracting

CITE THIS ARTICLE
Anurag K, Jangid P P, Marimuthu S, Gurav A M, Srikanth N, Mangal A K, Venkateshwarlu B, Shiddamallayya N. Identification and authentication of *Agnimantha* plant species used in Ayurveda on the basis of anatomical and molecular phylogenetic analysis. Plant Science Today (Early Access). https://doi.org/10.14719/pst.2180

Abstract

Agnimantha plant species have been used in the Ayurvedic system of medicine for many years and is widely used as an ingredient in many ayurvedic formulations. However, the source for *Agnimantha* remained controversial as it is difficult to authenticate from various reports. Hence, the present study aims to identify and authenticate its original and substitute sources. As per the literature sources *Clerodendrum phlomidis* L.f., *C. inerme* (L.) Gaertn. and *Premna serratifolia L.* are considered *Agnimantha* species. The anatomy of the above mentioned species confirmed the presence of patches of up to 20 cells in the sclerenchyma of the root cortex, while in the absence of sclerenchyma of the stem cortex, abundant chambered crystals were also present in the bark of the stem and root in *C. phlomidis* as compared to *C. inerme* and *P. serratifolia*. Phylogenetic analysis using chloroplast (*matK, trnH-psbA*) and nuclear markers (*ITS, rbcl*) also indicates the close relation between *C. inerme* and *P. serratifolia* and hence places them both in the same clade, though *C. phlomidis* is closely related to the other species but placed in the adjacent clade. Hence, the study concludes that anatomical as well as molecular phylogenetic analysis reflect close relation between *C. inerme* and *P. serratifolia*. while a distant relation with *C. phlomidis.*

Keywords

Anatomy; Molecular phylogeny; Ayurveda; *Agnimantha*

Introduction

The botanical identity of *Agnimantha*, which is one of the *Dashamula* plant species, is still controversial. Physicians (ayurvedic) from different regions of India considered the source plants for *Agnimantha* are *Premna serratifolia* L., *P. tomentosa* Willd, *P. mollissima* Roth, *P. coriacea* var. *villosa* (C.B.Clarke) A.Rajendren & P.Daniel, *Clerodendrum phlomidis* L.f. and *C. inerme* (L.) Gaertn. (1). There is no description of types of *Agnimantha* in ancient texts, i.e., Charaka Samhita and Sushruta Samhita. Some *Nighantus* have described two types -*Brihat Agnimantha* and *Kshudra Agnimantha* (2). *Premna serratifolia* is considered *Brihat Agnimantha* and *C. phlomidis* is considered *Kshudra Agnimantha*, whereas according to the Ayurvedic Pharmacopoeia of India, *C. phlomidis* is the original source plant to be considered in *Agnimantha* (3). Moreover, Ayurvedic Formulary of India (Part I) reported *C. phlomidis* as the authentic plant source of *Agnimantha* while *P. serratifolia* Willd and *P. mucronata* Roxb. are substitutes.

Agnimantha is one of major component in the ayurvedic system of medicines like Brahmarasayana, Chavanaprasha, Narayanataila and Gorocanadivati. In *Agnimantha,* roots and leaves are used as crude drugs (4). It is also used as ingredient in around 25 products i.e., Dasamula. In the list of 70 medicinal plant species of high trade sourced from tropical forests, roots of *P. serratifolia* and *C. phlomidis,* are also included (5). *P. serratifolia* is considered as threatened red listed species of IUCN (6).

Agnimantha leaves are used to reduce inflammation and pain, in the treatment of Arshsas for Avagaha Sweda (tub bath sudation, Panchkarma) (7). The leaves of *P. serratifolia* are used in the treatment of colic, rheumatism, neuralgia, etc. Whereas *C. phlomidis* is used in dyspepsia, dysentery, colic, debility, and neural disorders, and *P. latifolia* Roxb. has germicidal activity and is used in the treatment of dropsy, colitis, and boils (8, 9). The juice of *C. inerme* leaves is used for reducing muscular pain, rheumatoid arthritis, and stiffness of the legs (10). Documentation, including studies on authenticity and substitute sources for *Agnimantha,* is inadequately documented. Consequently, this led to a lack of transparency regarding the use of authentic *Agnimantha* as mentioned in ancient texts. But to be accepted globally along with safe and effective ayurvedic products, identification of the authentic botanical entity is important for regulatory compliance.

The micromorphological method for authentication of herbal formulations and crude drugs is one of the important steps in r standardization. *Premna serratifolia, C. inerme* and *C. phlomidis* are different species, but they are collectively known as *Agnimantha*. Though the taxonomic identification of plants can easily be done by their morphological characteristics, the same is difficult when they are in dried form as many of the characteristics of plant parts change after drying. In case where plant drugs are in crude drug form, molecular and pharmacognostic studies will be highly effective in determining their botanical identity.

Pharmacognostic studies of the root of *Agnimantha* (*P. serratifolia* and *C. phlomidis*) have already been carried out (11-14). Pharmacognostic studies on the leaves and stem of different sources used as *Agnimantha* are not available. In this regard, comparative pharmacognostic evaluation of the leaves of *P. serratifolia*, *C. phlomidis,* and *C*. *inerme* was taken into consideration to authenticate the substitution of these source plants for *Agnimantha*.

In molecular phylogeny, a short sequence of DNA is used for accurate identification and authentication of species, complementing the classical taxonomic methods (15). Though DNA barcoding has been effectively used for classifying animal species, the same approach should be used to discriminate among plant species. Mitochondrial genomes of plants reveal minimal nucleotide substitution and maximal chromosomal rearrangements. On the other hand, the nuclear genome of plants shows extensive gene duplication. Previous DNA barcoding studies of plants have suggested some plastid coding and non-coding regions, like *trnH-psbA, rbcL, matK, rpoC1, and rpoB,* as promising candidates (16-21). Nonetheless, the gradually evolving coding regions in the genome of plastids may not possess sufficient variation to categorize closely related plant species, which might lower their potential as efficient barcodes. This problem can be solved by analysing selected loci either in combination or individually. The recently evolved nuclear region, i.e., the nuclear *ITS* spacer from the ribosomal *ITS* gene has also been suggested as a promising barcode.

Materials and Methods

Plant material collection and storage

Root, stem, and leaf samples were collected from one plant of each species mentioned below available in the Medicinal Plants Garden, Regional Ayurveda Research Institute, Pune, Maharashtra (India). The herbarium of the plant specimens of *Clerodendrum phlomidis* (SVUBS 2220), *Clerodendrum inerme* (SVUBS 14151), and *Premna serratifolia* (SVUBS 4536) was prepared and deposited in the herbarium of the Institute (RARI, Pune). All the plant samples were thoroughly washed under running tap water and fixed in the plant fixative FAA (Formalin, Acetic Acid, Alcohol, 10%:5%:50% + 35% water) before sectioning of plant tissues.

Anatomical analysis

Dehydration of plant tissues was done in an ascending series of ethanol up to 100% for one hour in each ascending series of alcohol using Johansen's technique (22). Infiltration was done by keeping tissues in wax in an oven at 60°C for 1 h, where the wax melted and the samples sank slowly into it. The xylene-wax mixture was then replaced with a fresh amount of pure wax for 30 minutes in the oven. The samples were embedded into pure paraffin wax in moulds and allowed to set for 1 hour to solidify. Properly embedded samples were sectioned at 12-15 µm thickness with a rotary microtome (Wasewox, India). The sections were de-paraffinized and rehydrated in a descending series of ethanol and then stained with Haematoxylin (Himedia, India) and safranin using standard laboratory procedures (22). Each slide was washed in running tap water for 2 minutes, then slides were dehydrated in an ascending series of ethanol and absolute ethanol with gentle shaking and mounted in Canada Balsam (Himedia, India). Microscopic data and photomicrographs of characteristic features were taken from a light microscope (Olympus BX45, Japan) equipped with a digital camera.

DNA extraction, amplification and sequencing

Extraction of DNA was done from tender leaves using a modified kit-based technique (Qiagen, USA). The absence of a specific region as a universal plant barcode led to consideration of four genomic loci corresponding to *matK, rbcl, trnH-psbA,* and *ITS* for developing DNA barcodes based on literature. The sequence information for most of the above-mentioned loci was not available for *Clerodendrum* and *Premna* species, attempts were made to amplify three chloroplast and a nuclear DNA marker (Table 1) in three plants to be considered in *Agnimantha (C. phlomidis, C. inerme* and *P. serratifolia)*. Amplification of

Table 1. Details of the primers used for amplification of *ITS-5, matK* and *rbcl* genome regions.

Sl. No	Primer name	Sequences (5'-3')	Annealing temp. (°C)	Product size (bp)	Reference
1	Internal transcribed spacer *(ITS5)*	F-5'-GGAAGTAAAAGTCGTAACAAGG-3' R-5'-TCCTCCGCTTATTGATATGC-3'	55	550	[33]
2	Chloroplast maturase K *(Matk)*	F-5'-TAATTTACGATCAATTCATTC-3' R-5'-CTTCCTCTGTAAAGAATTC-3'	55	880	[34]
3	Ribulose bisphosphate carboxylase *(Rbcl)*	F-5'-ATGTCACCACAAACAGAGACTAAAGC-3' R-5'-GTAAAATCAAGTCCACCRCG-3'	55	670	[34]
4	*trnH-psbA*	F-5'-CGCGCATGGTGGATTCACAATCC-3' R-5'-GTTATGCATGAACGTAATGCTC-3'	65	300	[35]

the desired locus was accomplished by taking a final volume of 25µL (Table 2) and the amplicons were visualized on 1.2% agarose gel (23). The presence of sharp single bands was taken for further sequencing (24) analysis. Sequencing of the amplified regions was performed using the Sanger Sequencing method (Eurofns Genomics India, Pvt. Ltd. Company).

The extracted DNA was quantified on a biophotometer by taking absorbance at 260 and 280 nm to calculate A (260/280) (Eppendorf Biophotometer Plus, Hamburg, Germany). The concentration of DNA was 25 ng/µL and O. D was 1.8.

Table 2. Details of PCR reaction.

PCR Components	Quantity (µL)
Template DNA	5
PCR master mix	12.5
Forward primer	2
Forward primer	2
Nuclease free water	3.5
Total	**25**

PCR amplification

PCR amplification was conducted using (50-100) ng of genomic DNA as a template in a 25 µL of PCR mixture (Table 1) containing 12.5 µL of PCR master mix (2X), 10 µM forward and reverse primers (2µL each), 3.5 µL nuclease-free water. The PCR conditions for different primer pairs were given below (*rbcl* and *matK* (Table 3), *ITS* (Table 4) and *trnH-psbA* (Table 5). The amplified products were detected by 1.5% agarose gel electrophoresis in TAE buffer and visualized by using ethidium bromide on Gel documentation system (BIORAD, USA).

Table 3. Details of PCR program for *rbcl* and *matK*.

Initial Denaturation	94.0°C for 3 min	
Denaturation	94. 0°C for 1 min	
Annealing temperature	49.0°C for 2 min	*34 Cycles
Extension	72.0°C for 2 min	
Final Extension	72.0°C for 7 min	

Table 4. Details of PCR program for *ITS5*.

Initial Denaturation	94.0°C for 5 min	
Denaturation	94. 0°C for 30 sec	
Annealing temperature	50.0°C for 30 sec	*29 cycles
Extension	72.0°C for 30 sec	
Final Extension	72.0°C for 5 min	

Table 5. Details of PCR program for *trnH-psbA*.

Initial Denaturation	94.0°C for 5 min	
Denaturation	94. 0°C for 30 sec	
Annealing temperature	50.0°C for 30 sec	*29 cycles
Extension	72.0°C for 30 sec	
Final Extension	72.0°C for 5 min	

Analysis of DNA sequences

Chromatograms of each and every single sequence were verified, and poor-quality DNA sequence ends was trimmed before making contigs. 60% of the original read length were maintained after trimming the raw sequences, subject to the minimum average quality score of Q20. All single nucleotide variations were assessed and validated by aligning the chromatograms from both forward and reverse sequencing results. Sequences with 80% and above overlap were used for creating consensus sequences for all the amplicons. The sequence was checked using Chromas for specific base pairs and editing and consensus sequence formation Bioedit was used. Suitable sequences from all the individuals were assembled and aligned using CLUSTALW 1.83 (for multiple alignment). Conserved, parsimony, and variable informative sites were determined using MEGA 11. A phylogenetic tree was drawn using the maximum likelihood method through MEGA 11 software. Outgroups *Kalaharia uncinate* (AY307080.1), *Volkameria inermis* (MF063737.1), *Rotheca incisa* (KX115512.1), *Tectona grandis* (JX856965.1), *Tetraclea* sp. (AB586373.1), and *Tectona grandis* (MN814870.1) used in phylogenetic tree were obtained from NCBI.

Tectona grandis (MN814870.1) used in phylogenetic tree were obtained from NCBI.

Result

In the present study, molecular and pharmacognostic analysis of three plant species being contemplated as sources of *Agnimantha* have been carried out. *Premna serratifolia*, *Clerodendrum phlomidis* and *Clerodendrum inerme* belonging to Lamiaceae, are considered source plants for *Agnimantha*.

On analysis, the transverse section of the leaves showed parenchyma well differentiated into upper palisade and lower spongy tissues, the presence of a cuticle on the epidermis, and anomocytic stomata on the lower surface. The presence of prismatic crystals of Calcium oxalate was observed in two species except *P. serratifolia*. On analysis of T.S. through the midrib, it showed radially arranged protoxylem towards the upper epidermis and metaxylem towards the lower side of the vascular bundle. A specific microscopic description of the species is given below, along with the sequence analysis of the molecular markers amplified.

Microscopic description

Premna serratifolia L.

*Stem***:** A T.S. obtained from the stem showed a nearly circular outline. The epidermis of stems consists of a single layer cell. The secondary cortex is narrow and composed of patches of sclerenchyma alternating with compressed parenchymatous cells (Fig. 1C & 2F), particularly above the phloem. The thin layer of cork cells is composed of elongated lignified cells. The secondary phloem is composed of tangential zones containing sieve elements and companion cells, which alternate with axial parenchyma cells and are permeated by a network of phloem rays. Secondary phloem rays are both uniseriate and biseriate. Both uniseriate and multiseriate rays are composed mostly of square and upright cells throughout the body. Tangential multiples of 2-3 stone cells are also present in the secondary phloem after some intervals (Fig. 1C & 2F). Secondary xylem comprises rounded to oval-shaped vessels that are mostly solitary with a few radial multiples of 2-3 (Fig. 1A & C). The vessel diameter is 30 (20-40) um and the vessel length is 350 (250-500) µm. Perforation plates in vessels are simply rounded to oval with distinctly bordered alternate pits on their lateral walls (Fig. 1F & G). The axial parenchyma is scanty paratracheal. Fibers are thin-walled, septate with simple pits on radial walls. Rays are uniseriate to biseriate, composed of square and upright cells only throughout the body (Fig. 1E). Vessel ray pits are simple to round with a reduced border. Any kind of crystal or mineral deposition was not found in both

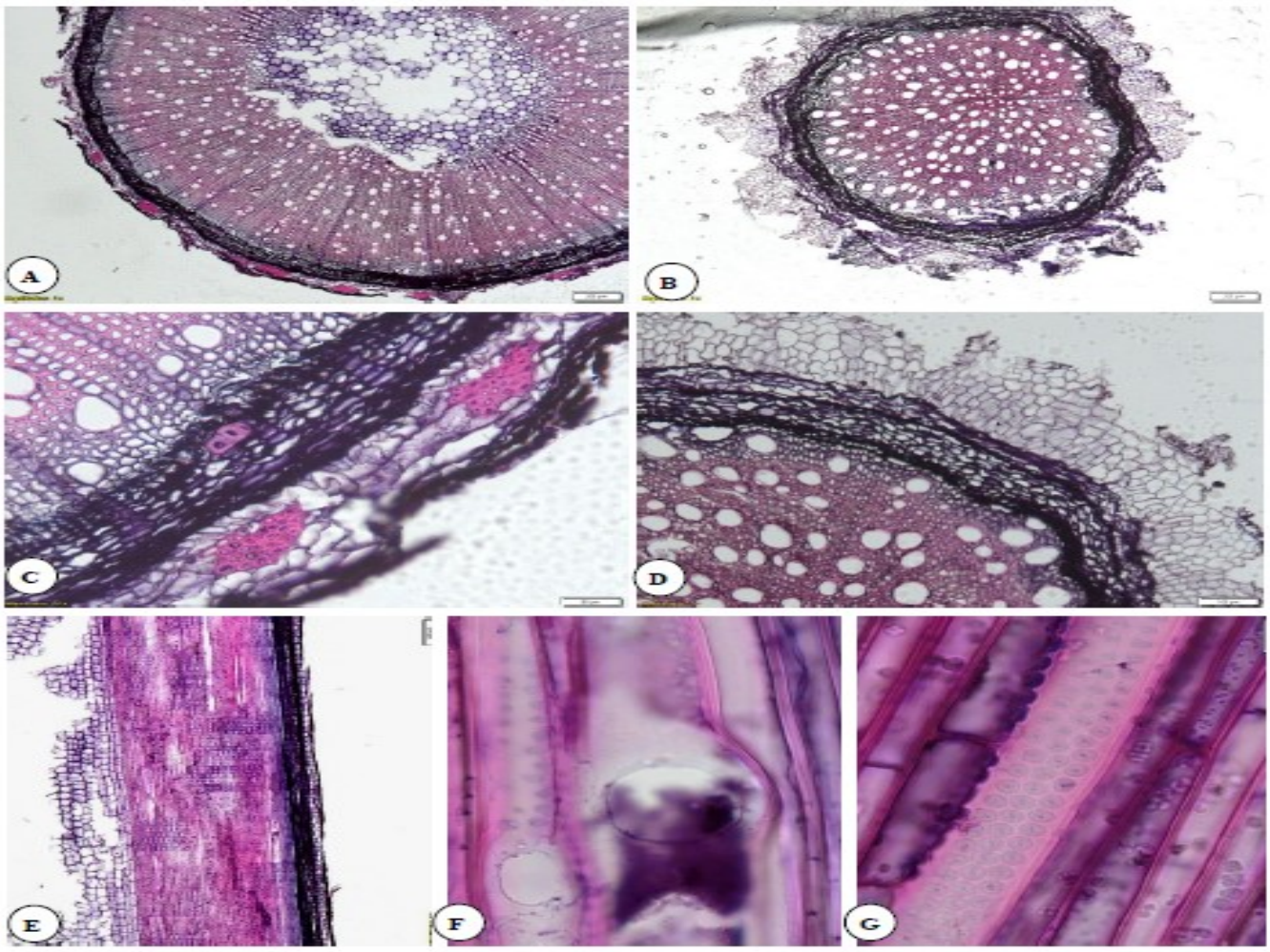

Fig. 1. *Premna serratifolia* L.: (A) T.S. of stem showing pith, xylem, phloem and bark structures X 4; (B) T.S. of root showing xylem, phloem and bark structures X 4; (C) T.S. showing cellular structure of stem bark containing stone cells and sclrenchyma fibre patches X 20; (D) T.S. showing root structure with bark X 10; (E) R.L.S. showing cellular composition of rays X 4; (F) R.L.S. showing simple perforation plates in vessels X 100; (G) R.L.S. showing alternate distinct bordered intervessel pitting on vessel element X 100.

xylem and phloem. A narrow pith made of parenchymatous cells is also present, followed by secondary xylem.

Root: The transverse section of the root is circular in outline, consisting of wavy cork cells followed by the cortex and vascular zone (Fig. 1B). The Cork layer is relatively thick in 4–6 layers of cells. The cortex is narrow and made up of thin-walled parenchyma. The xylem is well -developed and broader, measuring about three-fourths of the diameter of the cross-section. Xylem vessels with rounded to oval outlines are mostly solitary with few radial multiples of 2 or 3. The vessel diameter is 45 (25-70) um (Fig. 1D). Rays are conspicuous, both uniseriate and biseriate. Pith is absent in the mature stage of the root.

*Leaf***:** A transverse section of the petiole and midrib is composed of a single layered epidermis and cuboidal cells with cuticle thickening. The upper epidermis is followed by collenchyma cells (3-4 layers), and the cortical tissue is composed of numerous rows of parenchyma cells. Vascular bundles containing xylem and phloem were present in the centre of the midrib. The phloem is composed of parenchyma, sieve tubes, phloem rays, and phloem fibres. The xylem is composed of xylem vessels, fibers, wood parenchyma and xylem rays. Wood parenchyma containing elongated cells with pitted walls and spiral thickening was present on xylem vessels (Fig. 2A & C). At the centre, the ground tissue is made of parenchyma. The metaxylem occurs radially towards the periphery (abaxial surface), while the protoxylem occurs radially towards the centre (adaxial surface). Multicellular non-glandular and glandular peltate trichomes were present on both the upper and lower epidermis.

The transverse section of the leaf lamina showed the presence of both thickened upper and lower epidermis

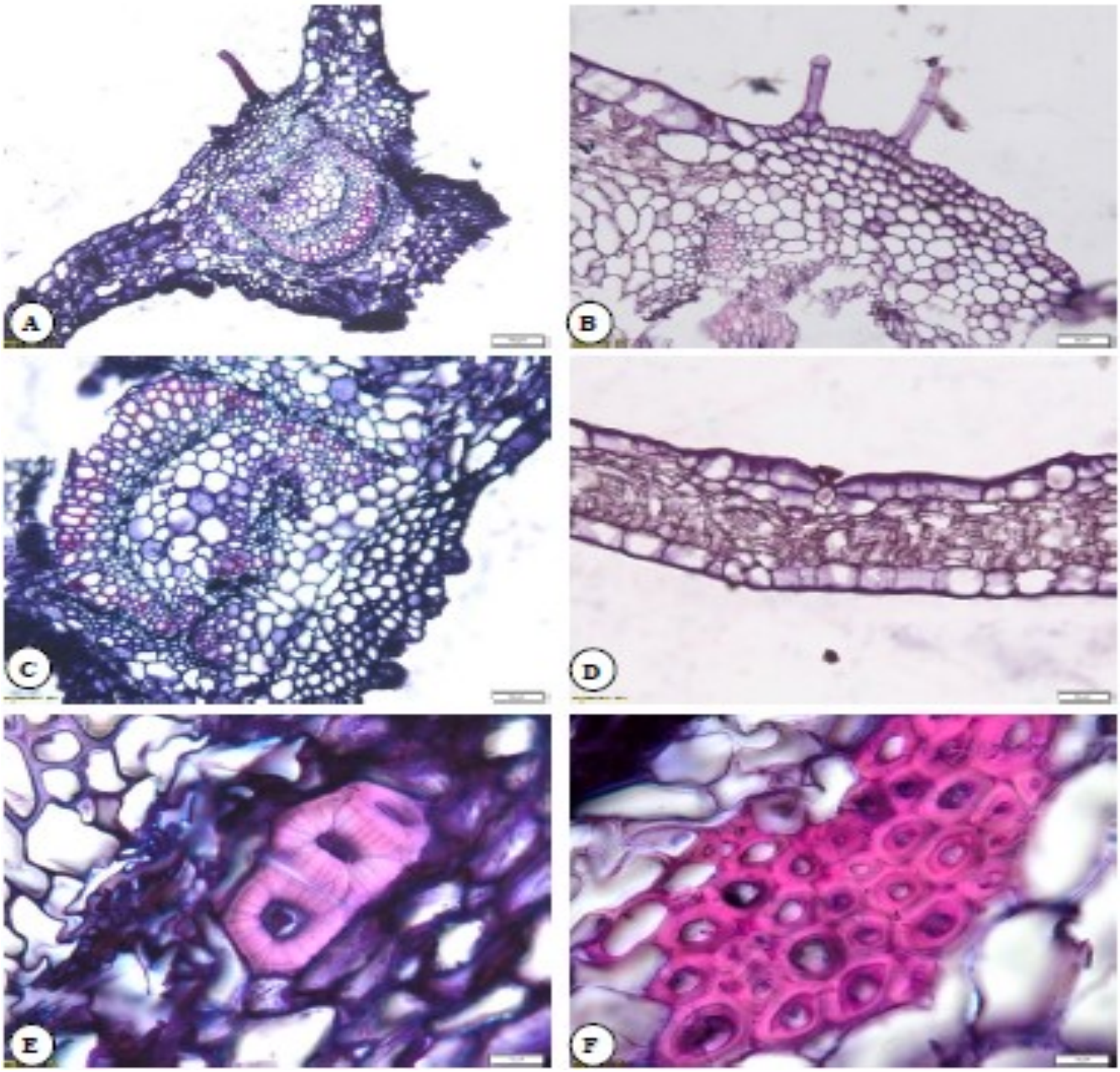

Fig. 2. ***Premna serratifolia*** **L.*:*** (A) T.S. of leaf through petiole with lamina X 10; (B) T.S. of leaf petiole showing nongladular covering trichomes X 20; (C) T.S. showing cellular structure of leaf petiole with vascular system X 20; (D) T.S. of leaf lamina showing cuboidal and rectangular cells in upper and lower epidermis with glandular trichome X 20; (E) T.S. of stem bark showing stone cells in secondary phloem X 100; (F) T.S. showing sclerenchyma fibres patches in stem bark X 100.

with cuticle. The upper and lower epidermis cells are big, rectangular, or cuboid-shaped. The lamina is characterized by the presence of single layers of palisade tissue that contain compact cylindrical parenchymal cells with green plastids on the dorsal surface. Spongy tissue comprises of 2-3 layers of spherical parenchyma with intercellular spaces on the ventral surface (Fig. 2D). The lower epidermis has two types of trichomes. The first is non-glandular multicellular covering trichomes. Meanwhile, the second is a glandular peltate consisting of a basal cell, and unicellular stalk and an 8-celled head (2-30 µm in diameter and 20 µm in length) that is a little bit sunken in the epidermis (Fig. 2B & D).

Clerodendrum inerme (L.) Gaertn.

Stem: The transverse section of the stem has a nearly circular outline containing glandular trichomes on the surface. The epidermis of stems consists of a single layer of cells broken at many places due to the pressure of cells produced by phellogen, forming a thin layer of elongated brown, lignified cork cells (Fig. 3A). Secondary cortex is composed of patches of sclerenchyma cells alternating with compressed parenchymatous cells, particularly above the phloem. The secondary phloem is composed of sieve elements and companion cells, which alternate with axial parenchyma cells. Small patches of up to 10 cells or tangential multiples of 4-5 sclerenchyma cells are also present in a ring in the secondary phloem after short intervals of parenchyma cells (Fig. 3C). Secondary phloem rays are uniseriate or 2-3 seriate. Both types of rays are composed mostly of square and upright cells throughout the body (Fig. 3E). Secondary xylem comprises rounded to angular vessels present mostly in radial multiples of 2-3 with some solitary vessels. Vessel diameter is 35 (30-45) µm and vessel length is 320 (211-403) µm. Perforation plates in vessels are generally simple and rounded, but reticulated perforation plates can be seen in combination with simple perforation plates at a few places (Fig. 3G). Inter-vessel pits are alternate and distinctly bordered. Vessel ray pits are simple to round with a reduced border.

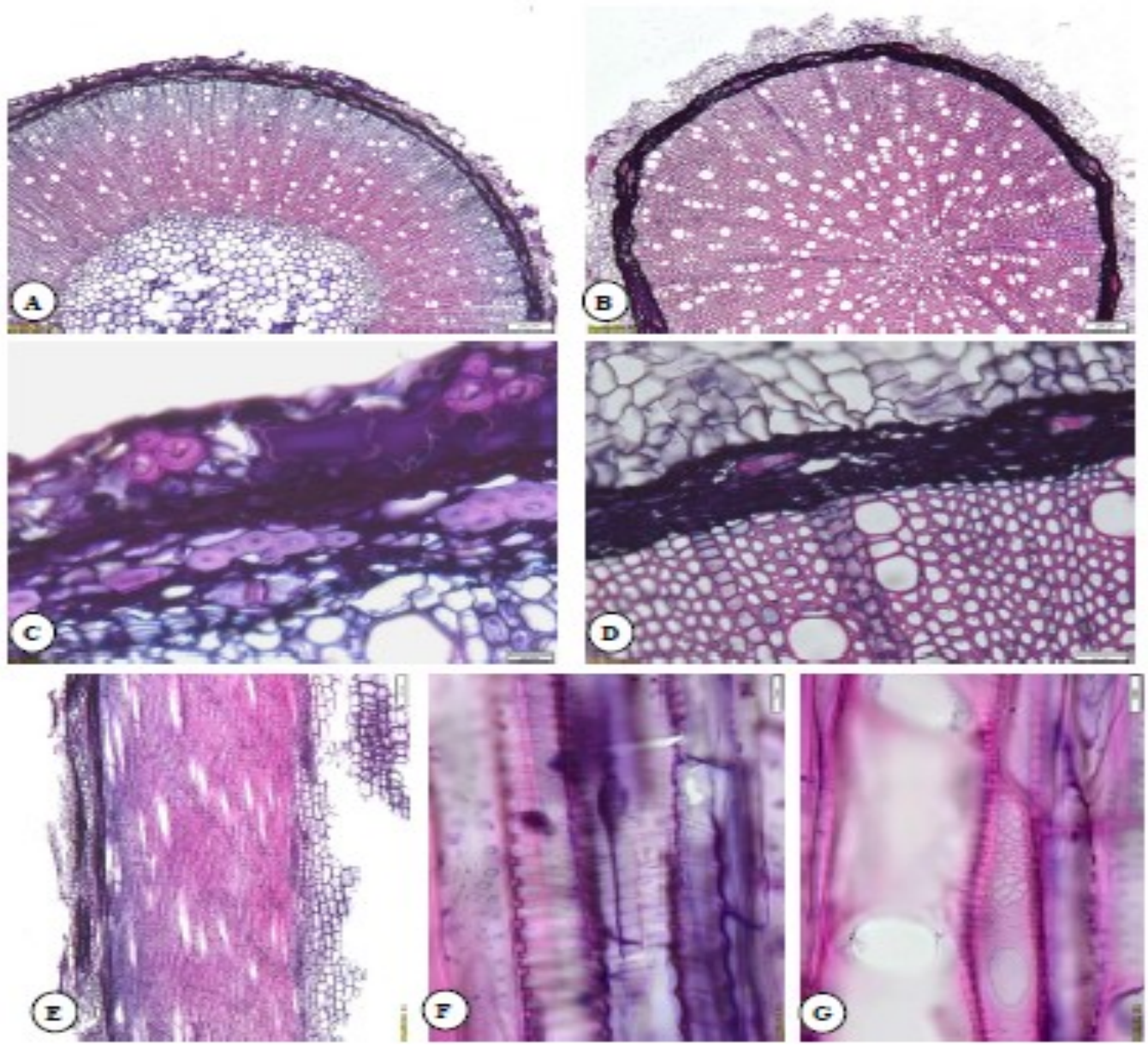

Fig. 3. *Clerodendrum inerme*: (A) T.S. of stem showing pith, xylem, phloem and bark X 4; (B) T.S. of root showing xylem, phloem and bark structure X 4; (C) T.S. showing cellular structure of bark containing sclerenchyma fibre patches X 40; (D) T.S. showing root structure with stone cells in root bark X 20; (E) R.L.S. showing rays and fibre cellular composition X 4; (F) R.L.S. showing helical thickening on fiber and vessel elements X 100; (G) R.L.S. showing perforation plates in vessels X 100.

The axial parenchyma is scanty paratracheal. Spiral thickening on vessel and fibre elements is also present near the pith region (Fig. 3F). Fibers are thin walled, septate with simple pits on radial walls. Rays are uniseriate to biseriate, composed of square and upright cells only throughout the body. A prismatic and rhomboidal crystal was found in the sclerenchyma cells of secondary phloem (Fig. 4E). A narrow pith made of parenchymatous cells is also present in the centre followed by secondary xylem.

Root: The transverse section of the root is circular in outline, consisting of 4-6 cells of layered cork followed by cortex and vascular zone (Fig 3B). The cortex is narrow, with stone cells scattered in thin-walled parenchyma. The secondary phloem is thin, containing tangential multiples of 2-3 stone cells after long intervals of parenchyma cells in a ring (Fig. 3D). Stone cells of the cortex as well as secondary phloem containing rhomboidal crystals in its lumens (Fig. 4F). The xylem is well-developed and wider, measuring about three-fourths of the diameter of the cross section. Xylem vessels are rounded to angular in outline, mostly in radial multiples of 2-4 with a few solitary vessels. The vessel diameter is 52 (34-65) µm. Rays are conspicuous, 1-3 seriate. Fibers are thin walled. The axial parenchyma is scanty paratracheal. Pith is absent.

*Leaf***:** The transverse section of the midrib and petiole contain epidermis in a single layer with thickened cuboidal cells. The upper epidermis was followed by collenchyma cells (2-3 layers), and the cortex was formed of several rows of parenchyma cells. Vascular bundle is present in the centre of the midrib. The phloem was composed of parenchyma sieve tubes and thin-walled fibres. Xylem was composed of vessels, wood parenchyma, and thin-walled fibers. The xylem vessels showed spiral thickening. Cortical tissue was made of parenchyma, which occupied its centre. The organization of protoxylem is pointed towards the adaxial surface, while it is on the abaxial

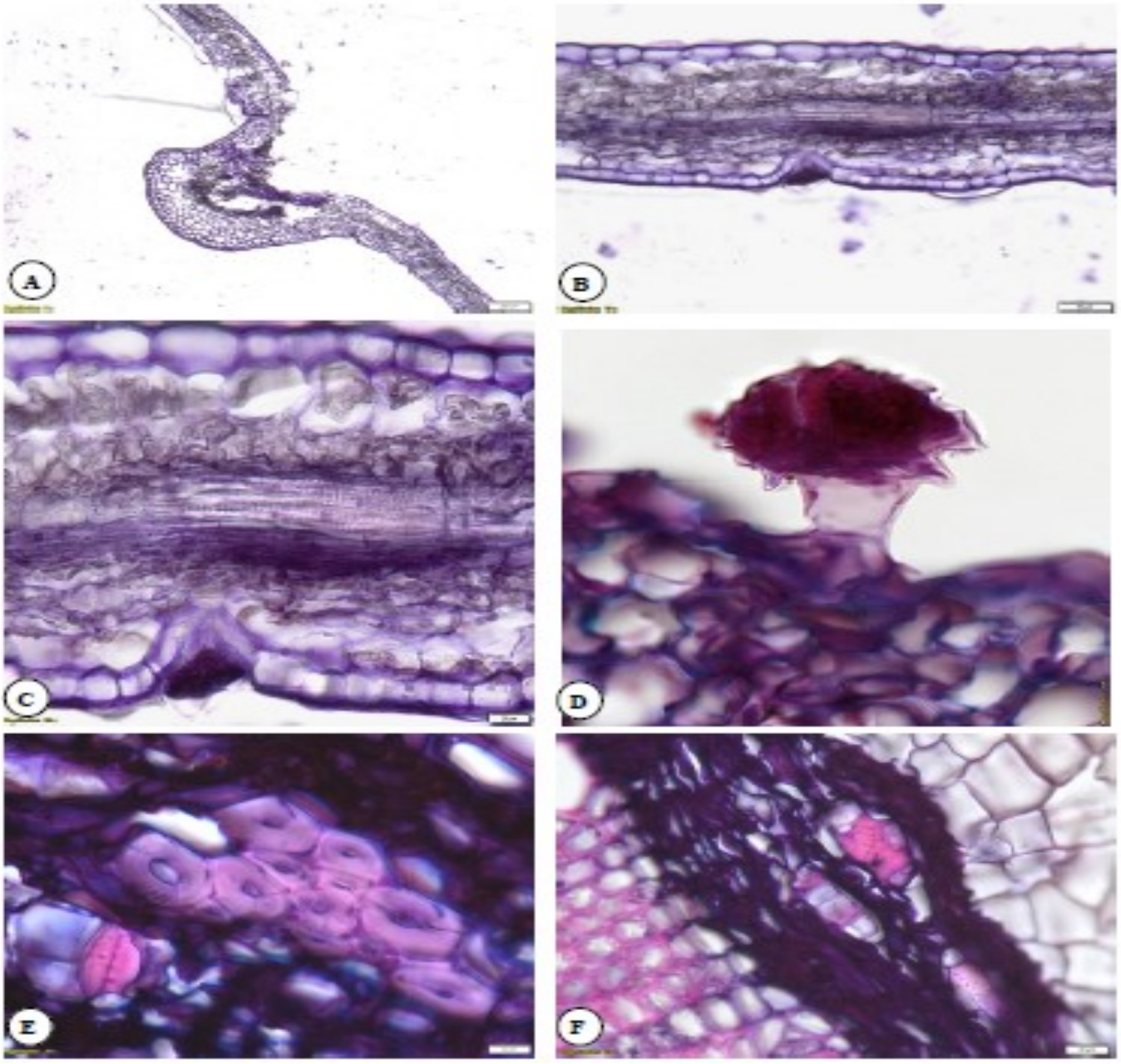

Fig. 4. *Clerodendrum inerme:* (A) T.S. of leaf showing through petiole with lamina X 4; (B) T.S. of leaf lamina showing cuboidal and rectangular cells of upper and lower epidermis X 20; (C) T.S. showing cellular structure of leaf lamina with vascular system and glandular trichome on lower epidermis X 40; (D) T.S. showing glandular peltate trichomes on leaf petiole X 100; (E) T.S. showing sclerenchyma fibers patches and crystals in bark of stem X 100; (F) T.S. showing crystals in stone cells of root bark X 40.

surface in the case of metaxylem. Glandular peltate types of trichomes exist on both the upper and lower epidermis (Fig. 4A).

In the cross-section of the leaf lamina, the upper and lower epidermises are made up of big, rectangular, or cuboid-shaped cells thickened with cuticle. The lamina is characterized by the presence of palisade and spongy layers on the dorsal and ventral surfaces, respectively. Below the upper epidermis, single layered compact cylindrical palisade tissue with green plastids is found in the midrib region (Fig. 4B). Spongy tissue comprises spherical parenchyma cells (2-3 layers) containing intercellular spaces. Non-glandular trichomes were very rare, and small (20-30 µm in length) on the upper epidermis only, while glandular trichomes (20 µm in length) are present on the lower epidermis. Glandular trichomes are a little bit sunken in the epidermis (Fig. 4D).

Clerodendrum phlomidis L.f.

*Stem***:** The transverse section of the stem revealed a nearly circular outline covered with non-glandular and glandular peltate trichomes (Fig. 6G). The epidermis of stems consists of a single layer cell. In the young stem, the bark is composed of a narrow secondary cortex composed of 4-5 rows of compressed parenchymatous cells. At maturity or after secondary growth, the epidermis broken out and 4-5 cork are formed by phellogen. The thin layer of cork cells is formed of elongated brown cells, or lignified cells. The secondary phloem is composed of tangential zones of sieve elements and companion cells with axial parenchyma cells. Secondary phloem rays may be uniseriate or biseriate. Small patches of 4-5 sclerenchyma cells are also present in the secondary phloem after some intervals in a ring. 1-2 celled layers of vascular cambium are present following secondary phloem (Fig. 5A & C). Secondary xylem comprises rounded to angular vessels that are mostly solitary with a few radial multiples of 2-3. Perforation plates in vessels are simple, rounded to oval, with distinctly bordered alternate pits on their lateral walls (Fig. 5F). The axial parenchyma is scanty paratracheal.

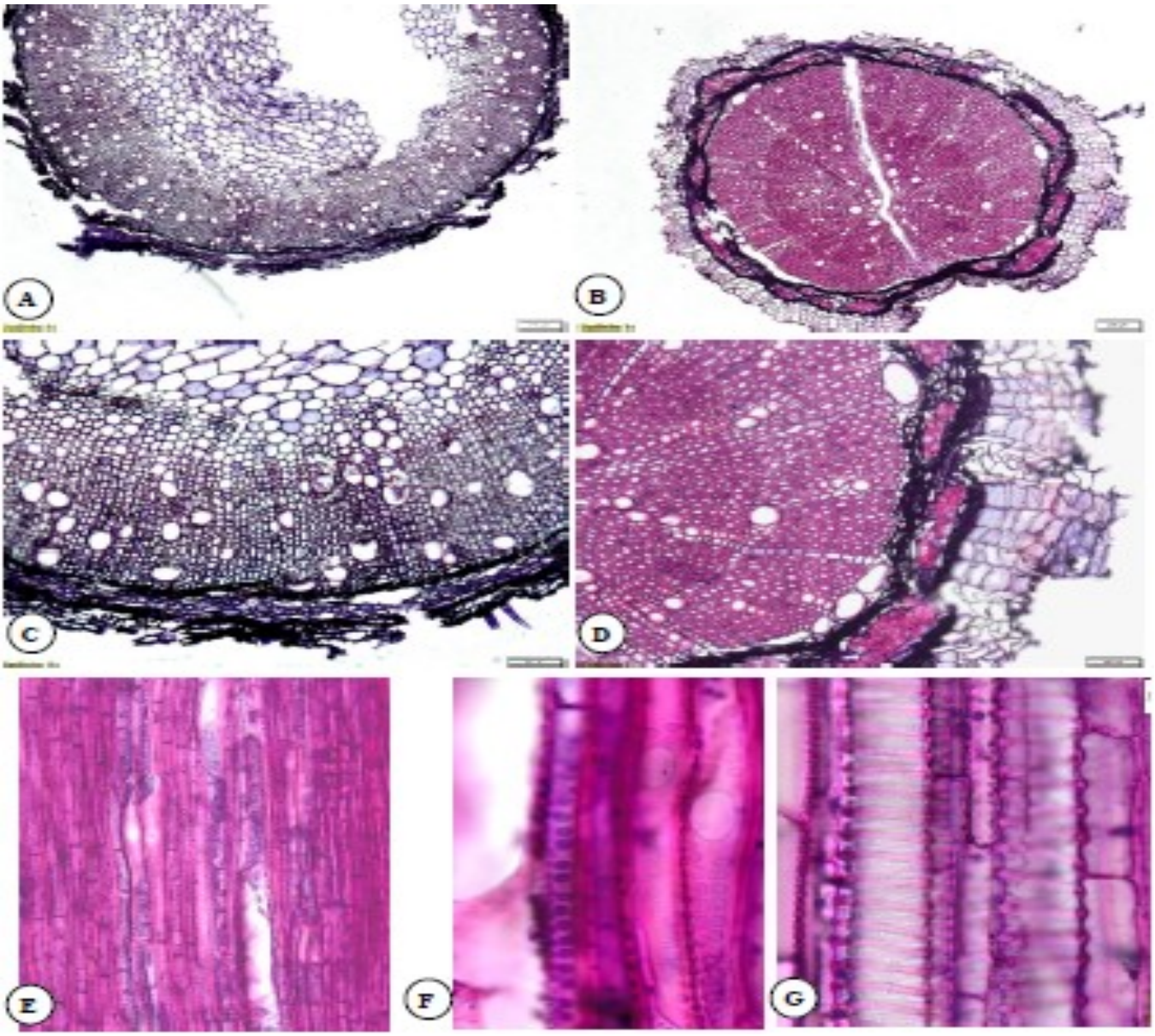

Fig. 5. **Clerodendrum Phlomidis**: (A) T.S. of stem showing pith, xylem, phloem and bark X 4; (B) T.S. of root showing xylem, phloem and bark structures X 4; (C) T.S. showing cellular structure of stem bark with trichomes X 10; (D) T.S. showing root structure X 10; (E) R.L.S. showing septate fibers with vessels X 10; (F) R.L.S. showing simple perforation plates in vessels X 100; (G) R.L.S. showing helical thickening on vessel elements X 100.

Fibers are thin walled, septate, with simple pits on radial walls. Rays are uniseriate to biseriate, composed of square and upright cells only throughout the body (Fig. 5E). Vessel ray pits are simple, rounded to horizontal/gash-like, with a reduced border. Abundant chambered prismatic / rhomboidal crystals are present in secondary phloem fibers (Fig. 6E & F). A well-developed pith of parenchymatous cells is also present in the centre followed by secondary xylem.

*Root***:** The transverse section of the root is circular in outline, consisting of 4-5 layers of cork cells, followed by the cortex and vascular zone. The secondary phloem is narrow with scattered sclerenchyma fiber patches of 5-6 cells, and the cambium is formed into a ring. The xylem is well-developed and wider, measuring about three-fourths of the diameter of the cross section. Xylem vessels with a rounded to oval outline, mostly solitary with a few radial or tangential multiples of 2 or 3 (Fig. 5B & D). Xylem fibers are thin to thick walled. Rays are conspicuous, both uniseriate and biseriate. Pith is absent in the mature stage of the root. Abundant chambered prismatic /rhomboidal crystals are present in the secondary phloem fibers (Fig. 6F).

*Leaf***:** The cross section of the petiole and midrib was convex on the adaxial surface with a single layered epidermis of cuboidal cells. Two or three layers of collenchyma cells were present below the upper epidermis. A collateral vascular bundle present in the centre of the midrib. Xylem and phloem were present in vascular bundles. The arrangement of the protoxylem and metaxylem was similar to that of *C. inerme* (Fig. 6A & C).

The cross-section of the lamina showed thickening of the cuticle on both the upper and lower epidermis. Both the epidermis cells consist of big, rectangular or cuboid-shaped cells. The lamina was characterized by the presence of palisade and spongy layers on the dorsal and ventral surfaces, respectively. A highly compact single layer of cylindrical cells of palisade tissue was present below the upper epidermis. One or two layers of spherical parenchyma cells containing intercellular spaces were present in spongy tissue (Fig. 6B). Both glandular and non-glandular trichomes were present on the epidermis. Non-

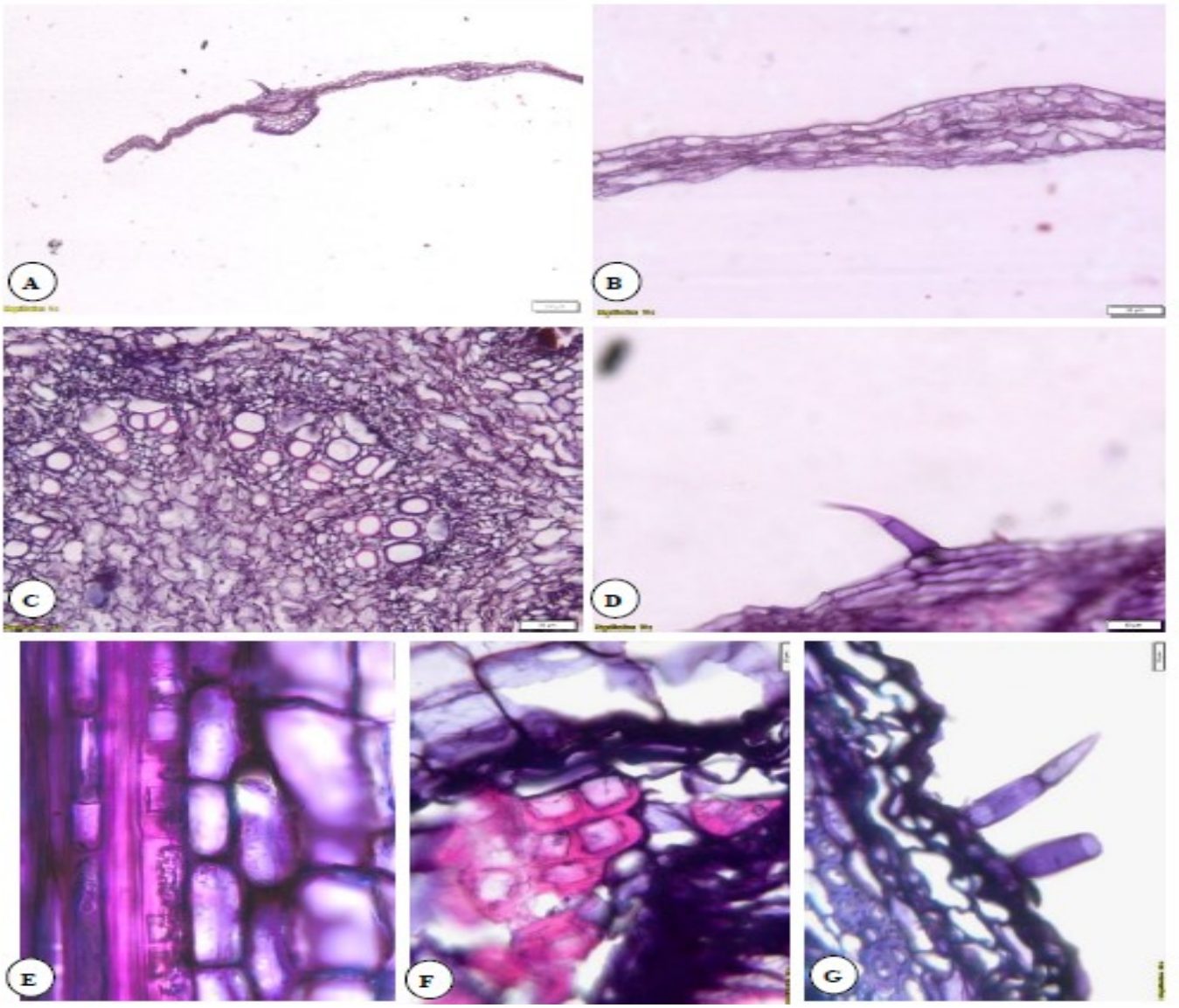

Fig. 6. ***Clerodendrum Phlomidis:*** (A) T.S. of leaf showing through petiole with lamina X 4; (B) T.S. of leaf lamina showing upper and lower epidermis X 20; (C) T.S. showing cellular structure of leaf petiole with vascular system X 20; (D) T.S. of petiole showing upper epidermis with trichome X 40; (E) R.L.S. showing chambered crystals in sclerenchyma fibers in stem bark X 100; (F) T.S. showing crystals in sclerenchyma fibers in root bark X 40; (G) T.S. of stem showing non-glandular covering trichome on the bark of stem X 40.

glandular multicellular trichomes were 50-140 µm in length and 20 µm in width (Fig. 6D). Meanwhile, glandular peltate trichomes with 20-30 µm length and 20-40 µm in width on both surfaces.

Dichotomous identification key for Agnimantha species:

1a. Vessels in stem are mostly in radial multiples of 2-3 with few solitary vessels, stone cells present in the root bark, perforation plates are both simple and reticulate……..…….…….…….....*C. inerme*

b. Vessels in stem are mostly solitary with few radial multiples of 2-3, perforation plates are exclusively simple, stone cells absent in root bark……..…..2

2a. Sclerenchyma fibres present in the stem cortex, absent in the secondary phloem of the stem and absent in the root bark, stone cells are present in the secondary phloem of the stem, crystals are absent in the root and stem bark, helical thickening is absent on vessels……..…….... ……..*P.serratifolia*

b. Sclerenchyma fibres are absent in the stem cortex, present in the secondary phloem of the stem and present in root bark, stone cells are absent, Abundant crystals are present in the root and stem bark, helical thickening is present on vessels……..

……..C. *phlomidis*

Molecular Analysis

The result obtained in the current study also helps in the generation of DNA barcoding for the above-mentioned species, as the markers used are well established for the generation of DNA barcodes especially *rbcl*, *matk, psba-trnH,* and *ITS* (25, 26). In molecular analysis, 3 chloroplast markers (*matK, rbcl and trnH-psbA*) and one nuclear marker (*ITS*) were used. Though we are unable to amplify *matk* as we have used the primer taken from a single position, it may be amplified using primers from different positions (loci). The isolated genomic DNA was used to amplify the markers, and single bands were obtained for *rbcl, trnH-psbA,* and *ITS* (Fig. 7) while no bands were observed in case of *matK* which signifies no amplification. PCR amplification and sequencing of bidirectional reads were the highest for *ITS* (99 %), followed by *rbcL* (98%), *trnH-psbA* (96.7%) and *matK* (0%). The amplified fragments were then purified and sequenced for further analysis, and a tree was constructed (Fig. 8, 9 and 10). The sequence obtained from Sanger sequencing was blasted using BLAST (https://blast.ncbi.nlm.nih.gov/Blast.cgi?

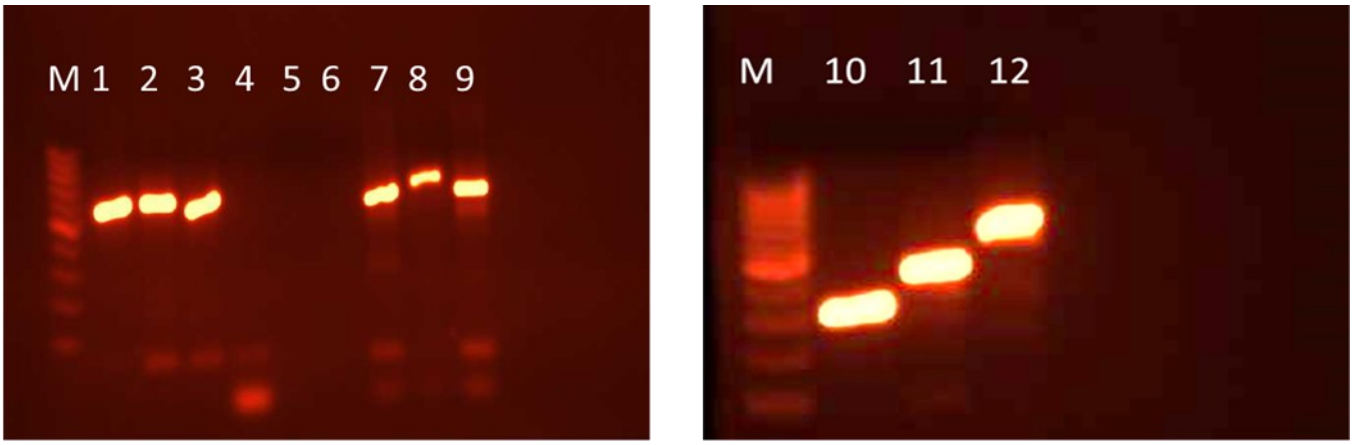

Fig. 7. Amplified markers on agarose gel (M=1 kb marker, lane 1, 2 and 3 representing *rbcl*; lane 4, 5 and 6 representing *matK*; lane 7, 8 and 9 representing *ITS*; lane 10, 11 and 12 representing *psba-trnH* in *C. phlomides*, *C. inerme* and *P. serratifolia L.* respectively)

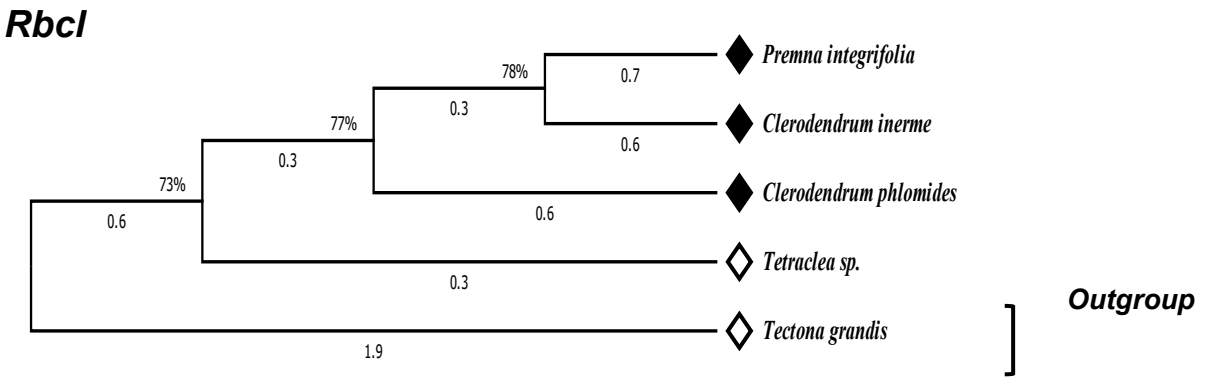

Fig. 8. The evolutionary history was inferred by using the Maximum Likelihood method and Tamura-Nei model [36, 37]. The tree with the highest log likelihood (-4057.61) is shown. Initial tree(s) for the heuristic search were obtained automatically by applying Neighbor-Join and BioNJ algorithms to a matrix of pairwise distances estimated using the Tamura-Nei model, and then selecting the topology with superior log likelihood value. The proportion of sites where at least 1 unambiguous base is present in at least 1 sequence for each descendent clade is shown next to each internal node in the tree. This analysis involved 5 nucleotide sequences. There were a total of 784 positions in the final dataset. Evolutionary analyses were conducted in MEGA11

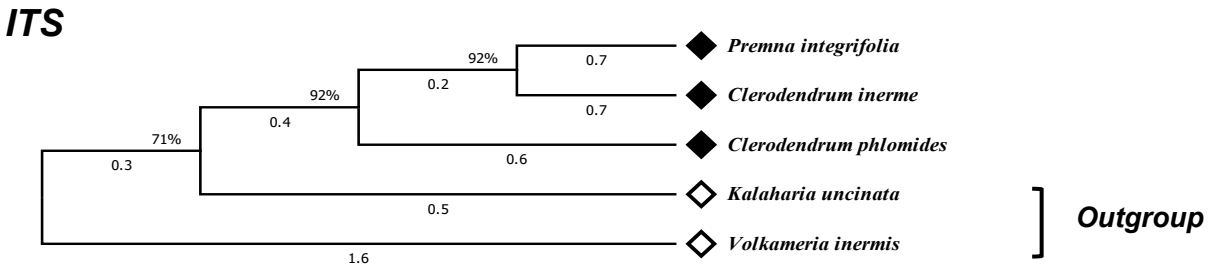

Fig. 9. The evolutionary history was inferred by using the Maximum Likelihood method and Tamura-Nei model [36, 37]. The tree with the highest log likelihood (-4596.40) is shown. Initial tree(s) for the heuristic search were obtained automatically by applying Neighbor-Join and BioNJ algorithms to a matrix of pairwise distances estimated using the Tamura-Nei model, and then selecting the topology with superior log likelihood value. The proportion of sites where at least 1 unambiguous base is present in at least 1 sequence for each descendent clade is shown next to each internal node in the tree. This analysis involved 5 nucleotide sequences. There were a total of 784 positions in the final dataset. Evolutionary analyses were conducted in MEGA11

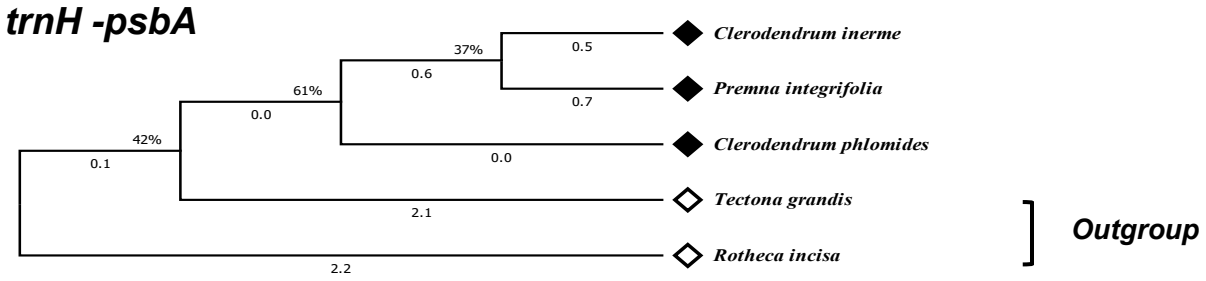

Fig. 10. The evolutionary history was inferred by using the Maximum Likelihood method and Tamura-Nei model [36, 37]. The tree with the highest log likelihood (-2628.22) is shown. Initial tree(s) for the heuristic search were obtained automatically by applying Neighbor-Join and BioNJ algorithms to a matrix of pairwise distances estimated using the Tamura-Nei model, and then selecting the topology with superior log likelihood value. The proportion of sites where at least 1 unambiguous base is present in at least 1 sequence for each descendent clade is shown next to each internal node in the tree. This analysis involved 5 nucleotide sequences. There were a total of 784 positions in the final dataset. Evolutionary analyses were conducted in MEGA11.

PAGE_TYPE=BlastSearch), NCBI and found more than 95% homogeneity. The phylogenetic tree constructed for all the markers (chloroplast and nuclear) depicts a close relationship between *C. inerme* and *P. serratifolia* and a distant relationship with *C. phlomidis* (Fig. 8, 9 and 10).

Discussion

Currently, increasing demand for herbal drugs leads to drug substitution and adulteration. Exponential exploitation of plant resources is being done to fulfil the needs and demands of herbal industries, which leads to a scarcity of plant resources. Thus, it is mandatory to document, authenticate, and validate the plant resources to maintain the quality of herbal products.

Various controversies are associated with the identification and usage of authentic plant species and plant parts in the case of *Agnimantha*. The existing literature reports different species of *Clerodendrum* and *Premna* in this group, but conclusions cannot be drawn for the correct identification. The differentiation between authentic and substitute sources of *Agnimantha* is still challenging. Phytochemical studies revealed that all three botanical sources possess varying amount of the marker compound verbascoside. Interestingly, the principle active compound was found to be higher in substitute sources such as *P. mollissima* and *P. serratifolia* than the authentic source *C. phlomidis,* leading to the possibility that *P. serratifolia* and *P. mollissima* could be the potential sources of *Agnimantha* (27).

There were a few molecular studies (28-31) already conducted on the species under study, but no reference was found regarding the relationship among these species. Similar studies on different varieties like Safed zeera adulteration in Kala zeera has been detected using molecular markers i.e., ITS2 and psbA-trnH. The amplified product of psbA-trnH barcode was different in Safed zeera (322 bp) as compared to kala zeera (257 bp) which can be easily resolved on agarose gel (32). However, morphological and anatomical studies reflect the relationship between these species on the basis of their external and structural features, but there is a lacuna in molecular based information. The current molecular phylogenetic and anatomical study involving the above-mentioned species plays a critical role in determining the authenticity of the source plant in the ayurvedic drug *Agnimantha*.

Anatomical characterization of the species involved revealed that all three species under the name *Agnimantha* are considerably similar in the anatomy of the root, stem, and leaves, except for some features. Though the species under study are closely related to each other, on the basis of differential anatomical features (Table 6) of these *Agnimantha* species, we can conclude that *C. inerme* is more closely related to *P. serratifolia* than to *C. phlomidis*. Moreover, the results of molecular analysis also corroborate the results obtained from anatomical studies

and suggest a close relationship between *P. serratifolia and C. inerme* and a distant relationship with *C. phlomidis. Clerodendrum phlomidis* is considered the authentic source of *Agnimantha*, while *P. serratifolia* and *C. inerme* are considered substitute sources as they possess equal morphological, anatomical, and phytochemical similarities with authentic species.

The results obtained in the present study are corroborated with the findings of API, but these are not enough to consider *C. inerme* and *P. serratifolia* as substitutes. Further Phytochemical and metabolomic based studies need to be conducted to authenticate the main source and substitutes.

Acknowledgements

The Director, RARI, Pune the Director General, CCRAS, New Delhi are duly acknowledged for the funding of this project. This study was funded by CCRAS, Ministry of Ayush, New Delhi, India.

Authors' contributions

AK - Carried out the molecular study and drafting of the manuscript. PPJ - Carried out the pharmacogenetic study and drafting of the manuscript. MS - Participated in designing of the experiment. AMG - PI of the Project, study design, planning of the study and proofreading of the manuscript. NS, AKM, BV, NS - Administrative coordination for the studies.

Compliance with ethical standards

Conflict of interest: Authors do not have any conflict of interests to declare.

Ethical issues: None.

References

1. Kamat SD, Kamat DK. Studies on medicinal plants and drugs in Dhanvantari-Nighaṇṭu.
2. Raja Nighantu, Indradeeva Tripathi. *Choukhambha orientalia*, Varanasi, Prabhadradi varga. 2003;pp.268.
3. Anonymous. The Ayurvedic Pharmacopoeia, Part 1, 1st edn, Vol. III, (Ministry of Health and Family Welfare, Department of Indian Systems of Medicine and Homoeopathy, Government of India). 2000;3(29):,147,178,209.
4. Vaidya BG. Nighantu adarsha. Chaukhambha Vidyabhavan. 1968;551-54.
5. Ved DK, Goraya GS. Demand and supply of medicinal plants. Medplant-ENVIS Newsletter on Medicinal Plants. 2008 Dec;1(1):2-4.
6. Razafiniary, V. *Premna serratifolia*. The IUCN Red List of Threatened Species. 2021: e.T66295794A68121996. https://dx.doi.org/10.2305/IUCN.UK.2021-1.RLTS.T66295794A68121996.en.
7. Agnivesha C Dridhabala, *Charaka samhita Chikitsha Sthana, Prameha Chikitshadhyaya.* 2001;6(47-48):2.
8. Agarwal VS. Rural economics of medicinal plants, vegetation in the forests. In: Drug plants of India. Kalyani Publishers, New Delhi. 1997;1(6):44.
9. Khare CP. Indian medicinal plants: an illustrated dictionary. *Springer Science* and Business Media. 2008 Apr 22; https://doi.org/10.1007/978-0-387-70638-2
10. Anonymous: Wealth of India. Council of Scientific and Industrial Research. 1948-76;2:67.
11. Kumar D, Kumar A, Prakash O. Pharmacognostic investigation of *Clerodendrum phlomidis* Linn. f. root. J Trop Life Sci. 2014 ;4(2):96-100. https://doi.org/10.11594/jtls.04.02.03
12. Sharma M, Raval N, Dave A, Shukla VD. Pharmacognostical evaluation of *Clerodendrum Serratum* (Linn.) Moon, (Bharangi) Root. Indian J Ancient Med Yoga. 2013 ;6(3):95.
13. Kumari HA, Shrikanth P, Pushpan RE, Harisha CR, Nishteswar K. Comparative pharmacognostical evaluation of leaves of regionally accepted source plants of *Agnimantha*. J Res Educ Indian Med. 2013;19(1-2):1-8.
14. Susan RS, Harini A, KN SK, Hegde PL. Pharmacognostic and phytochemical analysis of Agnimantha *(Premna corymbosa* Rottl.) leaf. J Ayurv Herb Med. 2016;1(2). https://doi.org/10.5530/jams.2016.1.14
15. Yang Z, Rannala B. Molecular phylogenetics: principles and practice. Nature Rev Genet. 2012;13(5):303-14. https://doi.org/10.1038/nrg3186
16. Group CP, Hollingsworth PM, Forrest LL, Spouge JL, Hajibabaei M, Ratnasingham S, van der Bank M, Chase MW, Cowan RS, Erickson DL, Fazekas AJ. A DNA barcode for land plants. Proc Nation Acad Sci. 2009;106(31):12794-97. https://doi.org/10.1073/pnas.0905845106
17. Li P, Qi ZC, Liu LX, Ohi-Toma T, Lee J, Hsieh TH, Fu CX, Cameron KM, Qiu YX. Molecular phylogenetics and biogeography of the mint tribe Elsholtzieae (Nepetoideae, Lamiaceae), with an emphasis on its diversification in East Asia. Scientific Reports. 2017;7(1):1-2. https://doi.org/10.1038/s41598-017-02157-6
18. Salmaki Y, Zarre S, Ryding O, Lindqvist C, Bräuchler C, Heubl G, Barber J, Bendiksby M. Molecular phylogeny of tribe Stachydeae (Lamiaceae subfamily Lamioideae). Mol Phylogenet Evol. 2013;69(3):535-51. https://doi.org/10.1016/j.ympev.2013.07.024
19. Scheen AC, Bendiksby M, Ryding O, Mathiesen C, Albert VA, Lindqvist C. Molecular phylogenetics, character evolution and suprageneric classification of Lamioideae (Lamiaceae) 1. Ann Missouri Bot Gard. 2010;97(2):191-217. https://doi.org/10.3417/2007174
20. Pham MP, Tran VH, Vu DD, Nguyen QK, Shah SN. Phylogenetics of native conifer species in Vietnam based on two chloroplast gene regions rbcL and matK. Czech J Genet Plant Breed. 2021;57(2):58-66. https://doi.org/10.17221/88/2020-CJGPB
21. Wattoo JI, Saleem MZ, Shahzad MS, Arif A, Hameed A, Saleem MA. DNA barcoding: amplification and sequence analysis of rbcl and matK genome regions in three divergent plant species. Advancements in Life Sciences. 2016;4(1):03-07.
22. Johansen D. A plant microtechnique, London: Mc Graw-Hill Book Company, Inc. 1940.
23. Veldman S, Ju Y, Otieno JN, Abihudi S, Posthouwer C, Gravendeel B, van Andel TR, de Boer HJ. DNA barcoding augments conventional methods for identification of medicinal plant species traded at Tanzanian markets. J Ethnopharmacol. 2020;250:112495. https://doi.org/10.1016/j.jep.2019.112495
24. Gogoi B, Wann SB, Saikia SP. DNA barcodes for delineating *Clerodendrum* species of North East India. Scientific Reports. 2020;10(1):13490. https://doi.org/10.1038/s41598-020-70405-3
25. Kress WJ. Plant DNA barcodes: Applications today and in the future. J Syst Evol. 2017;55(4):291-307. https://doi.org/10.1111/jse.12254
26. Li X, Yang Y, Henry RJ, Rossetto M, Wang Y, Chen S. Plant DNA barcoding: from gene to genome. Biol Rev. 2015;90(1):157-66. https://doi.org/10.1111/brv.12104
27. Vertuani S, Beghelli E, Scalambra E, Malisardi G, Copetti S, Toso RD, Baldisserotto A, Manfredini S. Activity and stability studies of verbascoside, a novel antioxidant, in dermo-cosmetic and pharmaceutical topical formulations. Molecules. 2011;16(8):7068-80. https://doi.org/10.3390/molecules16087068

28. Steane DA, Scotland RW, Mabberley DJ, Wagstaff SJ, Reeves PA, Olmstead RG. Phylogenetic relationships of *Clerodendrum* s.l. (Lamiaceae) inferred from chloroplast DNA. Syst Bot. 1997;229-43. https://doi.org/10.2307/2419455

29. Steane DA, Scotland RW, Mabberley DJ, Olmstead RG. Molecular systematics of *Clerodendrum* (Lamiaceae): ITS sequences and total evidence. Amer J Bot. 1999;86(1):98-107. https://doi.org/10.2307/2656958

30. Raj KA, Manimohan P. A new species and a new record of *Clitopilus* and a description of *C. orientalis* from India based on morphology and molecular phylogeny. Phytotaxa. 2018;343(1):47-59. https://doi.org/10.11646/phytotaxa.343.1.4

31. Ravikumar K, Ravichandran P. Taxonomy, pharmacognosy and phytochemical characteristics to identify the authentic and substitute botanical sources used as Agnimantha. Indian J Tradit Knowl. (IJTK). 2021;20(2):351-57. https://doi.org/10.56042/ijtk.v20i2.27806

32. Bansal S, Thakur S, Mangal M, Mangal AK, Gupta RK. DNA barcoding for specific and sensitive detection of *Cuminum cyminum* adulteration in *Bunium persicum*. Phytomedicine. 2018 ;50:178-83. https://doi.org/10.1016/j.phymed.2018.04.023

33. Issaravanich S, Ruangrungsia N, Palanuvej C, Vipunngeun N, Rungsihirunrat K. Microscopic, molecular and scopolamine content evaluations of *Datura metel* L. var. *metel* and *D. metel* L. var. *fastuosa* in Thailand. Res J of Pharmac Biolo Chem Sci. 2013;4:1009-21.

34. Sudmoon R, Chaveerach A, Tanee T. Analysis of genetics and chemical contents relation compared to commonly used *Cissus quadrangularis* L. and barcode markers of some Thailand *Cissus* species. Pakistan J Pharmac Sci. 2016;29(1):65-76.

35. Kress WJ, Wurdack KJ, Zimmer EA, Weigt LA, Janzen DH. Use of DNA barcodes to identify flowering plants. Proc Nation Acad Sci. 2005;102(23):8369-74. https://doi.org/10.1073/pnas.0503123102

36. Tamura K, Nei M. Estimation of the number of nucleotide substitutions in the control region of mitochondrial DNA in humans and chimpanzees. Molec Biol Evol. 1993;10(3):512-26.

37. Tamura K, Stecher G, Peterson D, Filipski A, Kumar S. MEGA6: molecular evolutionary genetics analysis version 6.0. Molec Biol Evol. 2013;30(12):2725-29. https://doi.org/10.1093/molbev/mst197